AIAA JOURNAL
Vol. 35, No. 12, December 1997

Postbuckling Analysis of Pultruded Composite Bars and Simple Frames

I. G. Raftoyiannis* and A. N. Kounadis†
National Technical University of Athens, 10682 Athens, Greece

A simplified but very reliable approach for the postbuckling analysis of pultruded composite bars and simple two-bar frames using the classical lamination theory is comprehensively presented. The overall postbuckling responses for symmetric I-structural shapes made from commercially available composite and homogeneous materials are thoroughly discussed. This leads to the optimum design of the structures under consideration. A simple stability criterion is also established for a direct determination of the critical loads. Two numerical examples are used to illustrate the simplicity and efficiency of the proposed procedure.

Nomenclature

A	= axial stiffness
A_{ij}	= extension stiffness terms
B_{ij}	= bending-extension coupling terms
b	= width
D	= bending stiffness
D_{ij}	= bending stiffness terms
d	= depth
E_f, ν_f, G_f	= fiber properties
E_m, ν_m, G_m	= matrix properties
$E_1, E_2, \nu_{12}, G_{12}$	= laminate properties
e	= eccentricity
k	= axial load
l	= beam length
Q_{ij}	= classical lamination theory (CLT) stiffness terms
$\bar{Q}_{ij}$	= transformed CLT stiffness terms
r_1, r_2	= elasticity modulus ratios
T_{ij}	= transformation matrix
t	= thickness
w	= lateral deflection
β	= nondimensionalized load
λ	= slenderness ratio
μ	= stiffness ratio
ξ	= axial displacement
ρ	= length ratio

Introduction

THE use of pultruded composite structural members such as beams and columns is spreading in modern engineering applications due to many advantages over conventional materials (steel, concrete, wood, etc.), such as the light weight in connection with high load-carrying capacity and high corrosion resistance. Mass production of composite structural members, e.g., by pultrusion, with open or closed thin-walled cross sections makes composite materials cost competitive with conventional ones. In the pultrusion process, fibers are pulled through a heated die that provides the cross-sectional shape to the final product. Pultrusion is a continuous process for prismatic sections of virtually any shape.[1] Other mass production techniques, such as automatic tape layout, can also be used to produce prismatic sections.

The overall buckling of composite columns[2] and simple frames is studied herein, whereas other types of failure, such as local buckling,[3] delamination, material degradation, etc.,[4–7] are not considered. For long composite columns, overall buckling is more likely to occur before any other instability failure, and the buckling equation has to account for the anisotropic nature of the material. For short columns, local buckling occurs first, leading either to large deflections and finally to overall buckling or to material degradation due to large deflections (crippling). The composite material is assumed to remain linearly elastic for deflections and strains larger than the ones of conventional materials corresponding to yield (steel) or crack (concrete). Therefore, failure of structures is mainly due either to elastic buckling (if they are imperfection sensitive) or to plastic buckling (if they exhibit postbuckling strength). For such a long composite column, the classical lamination theory (CLT)[8,9] is applied to determine the axial and bending stiffness of the column, which are next used for the study of its buckling and postbuckling behavior. Both stiffnesses can be obtained experimentally from full-size tests[10] or by considering each part of the cross section (flange and web) as an orthotropic plate with properties determined by coupon testing.[11]

Although pultruded members are not manufactured by lamination, they do contain different material combinations through the thickness, thus justifying the use of lamination theory. According to this theory, each layer is modeled as a homogeneous equivalent material that macroscopically behaves similarly to the fibrous composite. Next, CLT is used to model an entire flange or web as a yet equivalent homogeneous material. Flanges and web can be dealt with separately. The member stiffnesses can be derived either from the corresponding plate stiffnesses according to CLT or by reformulating CLT. Subsequently, efficient and readily employed buckling analyses of composite columns and simple two-bar frames with composite members,[2,12] both consisting of I-structural shapes made from commercially available composite and homogeneous materials, are comprehensively presented. Once the axial and bending stiffnesses of the bars are determined, the subsequent buckling[13] and postbuckling analyses are those reported in Refs. 14–17.

The present study was motivated by an actual problem. It is intended to help the engineer who is familiar with the postbuckling analysis of columns and frames made from homogeneous and isotropic materials to extend the field of application in the area of composite structures and vice versa.

Beam Stiffness from Classical Lamination Theory

Using CLT, the stiffness components of an anisotropic laminated plate (e.g., the flange or web of an I section) can be readily determined. Indeed, the constitutive equation for a laminate in matrix form is[8,9]

$$\begin{Bmatrix} \{N\} \\ \{M\} \end{Bmatrix} = \begin{bmatrix} [A] & [B] \\ [B] & [D] \end{bmatrix} \begin{Bmatrix} \{\varepsilon\} \\ \{\kappa\} \end{Bmatrix} \tag{1}$$

where $\{N\}$ and $\{M\}$ are the in-plane forces and moments, whereas $\{\varepsilon\}$ and $\{\kappa\}$ are the strains and curvatures, respectively. The elements

Received Nov. 19, 1996; revision received Aug. 4, 1997; accepted for publication Aug. 27, 1997.

*Postdoctoral Associate, Civil Engineering Department, 42 Patission Street.

†Professor, Civil Engineering Department, 42 Patission Street. Associate Fellow AIAA.

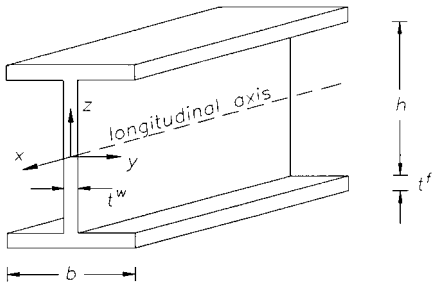

a) Structural shape and coordinate system

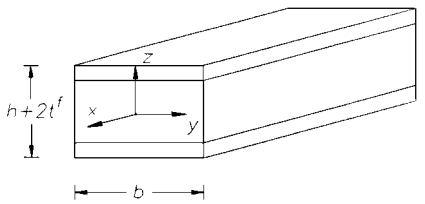

b) Equivalent laminate

Fig. 1 Typical I beam.

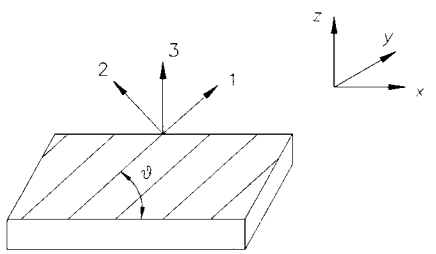

a) Flange

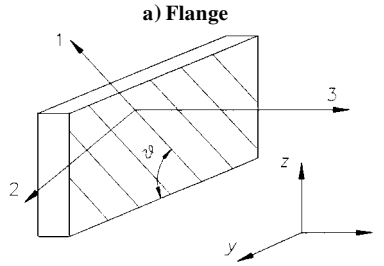

b) Web

Fig. 2 Material (1-2-3) and structural (x, y, z) coordinate system.

A_{ij}, B_{ij}, and D_{ij} of the matrices $[A]$, $[B]$, and $[D]$ are defined for a flange of thickness $t = t^f$ and width b (Fig. 1) as

$$(A_{ij}, B_{ij}, D_{ij}) = \frac{1}{b}\int_{-b/2}^{b/2}\int_{-t/2}^{t/2} \bar{Q}_{ij}(1, z, z^2)\,\mathrm{d}y\,\mathrm{d}z$$

$$= \int_{-t/2}^{t/2} \bar{Q}_{ij}(1, z, z^2)\,\mathrm{d}z \tag{2}$$

and for a web of a thickness $t = t^w$ and depth h as

$$(A_{ij}, B_{ij}, D_{ij}) = \frac{1}{t}\int_{-t/2}^{t/2}\int_{-h/2}^{h/2} \bar{Q}_{ij}(1, 0, z^2)\,\mathrm{d}y\,\mathrm{d}z$$

$$= \left(\frac{h}{t}, 0, \frac{h^2}{12t}\right)\int_{-t/2}^{t/2} \bar{Q}_{ij}\,\mathrm{d}y \tag{3}$$

where $\bar{Q}_{ij}$ is given by $\bar{Q}_{ij} = T_{ij}Q_{ij}$. The stiffness terms are $Q_{11} = E_1/(1-\nu_{12}\nu_{21})$, $Q_{22} = E_2/(1-\nu_{12}\nu_{21})$, $Q_{12} = \nu_{21}E_1/(1-\nu_{12}\nu_{21})$, and $Q_{66} = G_{12}$, and the material axes are defined in Fig. 2. Clearly, for symmetric laminates, the bending-extensional coupling effect B_{ij} is zero. The units for A_{ij}, B_{ij}, and D_{ij} are kilo-Newtons per meter, kilo-Newtons, and kilo-Newton meters, respectively. In using this approach, the web of an I beam (Fig. 1a) is transformed to an equivalent (rectangular) laminate of width b and depth h by introducing a width correction factor t^w/b (see Fig. 1b). Applying the parallel axis theorem[9] with respect to the midsurface of the cross section, one can establish a constitutive matrix for the whole cross section. For a symmetric I beam of flange width b and depth $h+2t^f$, the total stiffness components are

$$A_{ij} = (t^w/b)A_{ij}^w + 2A_{ij}^f$$
$$D_{ij} = (t^w/b)D_{ij}^w + 2D_{ij}^f + 2[(h+t^f)/2]^2 A_{ij}^f \tag{4}$$

where the superscripts f and w denote quantities referring to web and flange, respectively. Note that symmetry involves both geometry and material symmetry with respect to the middle surface, and hence the bending-extension coupling terms vanish ($B_{ij} = 0$).

So far, the analysis is similar to that of Vinson and Sierakowski[18] or Tsai[19] and is valid for a plane strain situation in the y direction (Fig. 1). The reduced stiffnesses Q_{ij} are obtained using CLT,[8] which assumes plane stress through the thickness of the flanges or web (Fig. 1). However, a plane stress assumption must be used through the width of the beam,[20] i.e.,

$$N_y = N_{xy} = 0$$
$$M_y = M_{xy} = 0 \tag{5}$$

Using Eqs. (5), the constitutive equation (1) yields

$$N_x^{\mathrm{tot}} = N_x b = A\varepsilon_x$$
$$M_x^{\mathrm{tot}} = M_x b = D\kappa_x \tag{6}$$

where

$$A = \left[A_{11} + \frac{2A_{16}A_{26}A_{12} - A_{66}A_{12}^2 - A_{22}A_{16}^2}{A_{22}A_{66} - A_{26}^2}\right]b \tag{7}$$

$$D = \left[D_{11} + \frac{2D_{16}D_{26}D_{12} - D_{66}D_{12}^2 - D_{22}D_{16}^2}{D_{22}D_{66} - D_{26}^2}\right]b \tag{8}$$

Barbero and Raftoyiannis[3] presented a similar expression valid for the bending stiffness of cross sections. In unidirectional composites, all fibers have a specific orientation in the matrix for each particular layer. A special case occurs when the fibers are randomly oriented in the matrix. The composite acts as a plane-isotropic material, and the properties were obtained using the following formulas[21]:

$$E = \tfrac{3}{8}E_1 + \tfrac{5}{8}E_2, \qquad G = \tfrac{1}{8}E_1 + \tfrac{1}{4}E_2, \qquad \nu = (E/2G) - 1 \tag{9}$$

The I-beam cross section of Fig. 3 is used as a model.

Nonlinear Buckling of a Simply Supported Bar

Consider the equilibrium in the slightly deformed configuration of the axially compressed bar shown in Fig. 4. It is assumed that the bar is of an I-structural shape made from composite material. The condition of equality of external and internal bending moments at any cross section yields

$$Dw''\left(1 + \tfrac{1}{2}w'^2\right) + Pw = 0 \qquad (D = EI) \tag{10}$$

or

$$w''\left(1 + \tfrac{1}{2}w'^2\right) + k^2 w = 0 \qquad (k^2 = P/D) \tag{11}$$

where the approximate nonlinear bending moment–curvature relation $M = -Dw''(1 + \frac{1}{2}w'^2)$ has been used.[22] Clearly, after neglecting the small term $\frac{1}{2}w'^2$ (compared with 1), Eq. (11) reduces to the well-known linear buckling equation. The integration of Eq. (11) is performed by using an efficient approximate analytical technique presented by Kounadis.[23] According to this technique, the last equation is written as follows:

$$w'' + k^2 w = -\tfrac{1}{2}w'^2 w'' \tag{12}$$

Introducing into the right-hand side of this equation the linear solution (where δ = middle span deflection)

$$w(x) = \delta \sin(\pi x/l) \tag{13}$$

we obtain the differential equation

$$w'' + k^2 w = \tfrac{1}{2}(\pi/l)^4 \delta^3 \cos^2(\pi x/l)\sin(\pi x/l) \tag{14}$$

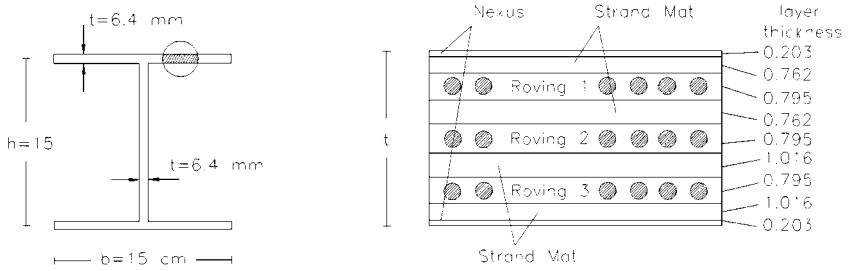

a) Flange

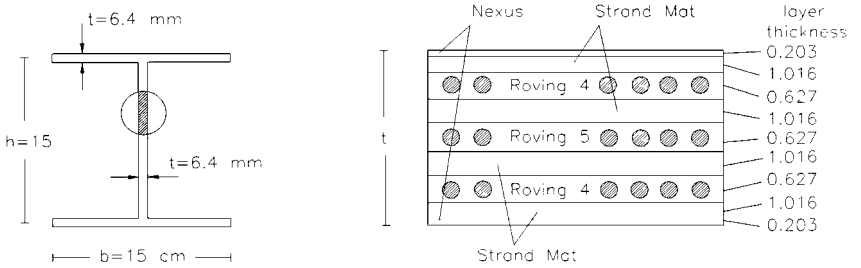

b) Web

Fig. 3 Layup for the 15 × 15 cm I beam.

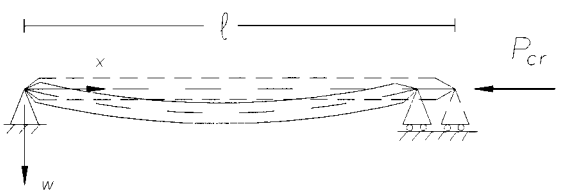

Fig. 4 Sign convention of simply supported bar under axial compression before and after buckling.

which, using trigonometric identities, may be written as

$$w'' + k^2 w = \tfrac{1}{8}(\pi/l)^4 \delta^3 [\sin(\pi x/l) + \sin(3\pi x/l)] \tag{15}$$

The general integral of this equation is given by

$$w(x) = w_h(x) + w_p(x) \tag{16}$$

where $w_h(x)$ is the solution of the homogeneous differential equation, i.e.,

$$w_h(x) = C_1 \sin kx + C_2 \cos kx \tag{17}$$

whereas $w_p(x)$ is the particular solution, i.e.,

$$w_p(x) = \frac{1}{8}\left(\frac{\pi}{l}\right)^4 \delta^3 \left[\frac{1}{k^2 - (\pi^2/l^2)} \sin\frac{\pi x}{l} + \frac{1}{k^2 - (9\pi^2/l^2)} \sin\frac{3\pi x}{l}\right] \tag{18}$$

The integration constants C_1 and C_2 are determined using the boundary conditions

$$w(0) = 0, \qquad w(l) = 0 \tag{19}$$

and are found to be

$$C_1 = 0, \qquad C_2 = 0 \tag{20}$$

Hence, the approximate solution of Eq. (15) is

$$w(x) = \frac{1}{8}\left(\frac{\pi}{l}\right)^4 \delta^3 \left[\frac{1}{k^2 - (\pi^2/l^2)} \sin\frac{\pi x}{l} + \frac{1}{k^2 - (9\pi^2/l^2)} \sin\frac{3\pi x}{l}\right] \tag{21}$$

which for $x = l/2$ yields

$$w\left(\frac{l}{2}\right) = \delta = \frac{1}{8}\left(\frac{\pi}{l}\right)^4 \delta^3 \left\{\frac{8\pi^2 l^2}{[k^2 - (\pi^2/l^2)][k^2 - (9\pi^2/l^2)]}\right\} \tag{22}$$

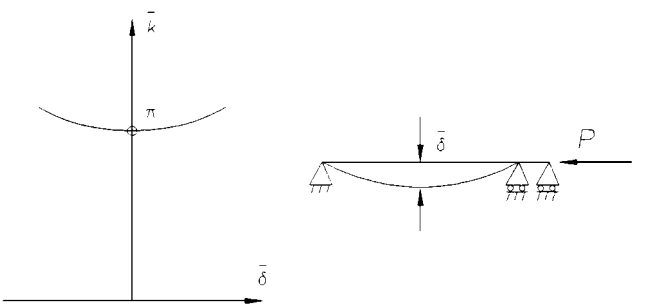

Fig. 5 Stable symmetric bifurcation point implying postbuckling for a simply supported bar under axial compression.

or

$$\bar{\delta} = (1/\pi^3)\sqrt{(\bar{k}^2 - \pi^2)(9\pi^2 - \bar{k}^2)} \tag{23}$$

where $\bar{\delta} = \delta/l$, $\bar{k} = kl$, and $\pi < \bar{k} \ll 3\pi$. A graphical representation of the postbuckling equilibrium path ($\bar{k}$ vs $\bar{\delta}$) is shown in Fig. 5. The secondary path has a horizontal tangent at the critical bifurcation point ($\bar{\delta}_{cr} = 0$ and $\bar{k}_{cr} = \pi$), which is stable symmetric. Of course, due to the approximation made, the range of application of the preceding formula must be restricted to values higher than $\bar{k}^2/\pi^2$ for which $\tan^{-1} w'(x) < 0.10$ rad.

Nonlinear Buckling of a Two-Bar Frame

The postbuckling analysis that follows assumes geometrically perfect members of I-structural shape made from linearly elastic composite material that may undergo moderate rotations but small strains. If such a member of length l, axial stiffness A (equivalent to EA), and bending stiffness D (equivalent to EI) is subjected simultaneously to bending and axial compression, the following elastic strain energy functional can be written:

$$U = \frac{1}{2}\int_0^l \left[A\left(u' + \frac{1}{2}W'^2\right)^2 + DW''^2\right] dx \tag{24}$$

where W and u are the lateral deflection and axial displacement of the centerline of the member, respectively. Introducing the nondimensionalized quantities $x = X/l$, $\xi = u/l$, $w = W/l$, and $\lambda^2 = Al^2/D$, the preceding equation is brought in a dimensionless form as follows:

$$\bar{U} = \frac{Ul}{D} = \frac{1}{2}\int_0^l \left[\lambda^2\left(\xi' + \frac{1}{2}w'^2\right)^2 + w''^2\right] dx \tag{25}$$

Let us now consider the two-bar frame, shown in Fig. 6, that is subjected to a compressive force P applied at its joint, eccentrically

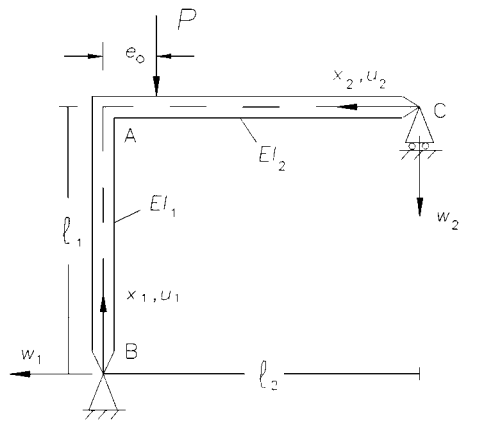

Fig. 6 Geometry and sign convention of a two-bar frame BAC subjected to a joint load *P* eccentrically applied to the centerline of the bar AB.

to the centerline of the column by e_0. Then, using Eq. (25), the total potential energy of the frame in dimensionless form is given by

$$U^T = \frac{1}{2}\int_0^1 \left[\lambda_1^2\left(\xi_1' + \frac{1}{2}w_1'^2\right)^2 + w_1''^2\right] dx_1 + \frac{\mu}{2\rho}\int_0^1 \left[\lambda_2^2\left(\xi_2' + \frac{1}{2}w_2'^2\right)^2 + w_2''^2\right] dx_2 + \beta^2\rho e w_2'(1) + \beta^2\rho e\xi_1(1) = 0 \tag{26}$$

where $\mu = D_2/D_1$, $\rho = l_2/l_1$, $\beta^2 = Pl_1^2/D_1$, and $e = e_0/l_2$. The principle of stationary total potential energy leads to the following differential equations[17,23]:

$$\lambda_1^2\left(\xi_1' + \tfrac{1}{2}w_1'^2\right)' = 0 \tag{27}$$

$$\lambda_2^2\left(\xi_2' + \tfrac{1}{2}w_2'^2\right)' = 0 \tag{28}$$

$$w_1'''' - \lambda_1^2\left[\left(\xi_1' + \tfrac{1}{2}w_1'^2\right)w_1'\right]' = 0 \tag{29}$$

$$w_2'''' - \lambda_2^2\left[\left(\xi_2' + \tfrac{1}{2}w_2'^2\right)w_2'\right]' = 0 \tag{30}$$

The boundary conditions associated with the preceding equations are

$$w_1(0) = \xi_1(0) = w_2(0) = 0 \tag{31}$$

$$w_1(1) = \rho\xi_2(1) \tag{32}$$

$$\xi_1(1) = -\rho w_2(1) \tag{33}$$

$$w_1'(1) = w_2'(1) \tag{34}$$

$$\xi_2'(0) + \tfrac{1}{2}w_2'^2(0) = 0 \tag{35}$$

$$w_1''(0) = w_2''(0) = 0 \tag{36}$$

$$w_1''(1) + (\mu/\rho)w_2''(1) + \beta^2\rho e = 0 \tag{37}$$

$$w_1'''(1) + k^2 w_1'(1) = 0 \tag{38}$$

$$(\beta^2 - k^2)\rho^2 + \mu w_2'''(1) = 0 \tag{39}$$

where $k^2 = Sl_1^2/D_1$; S is the axial compressive force in the column. Integration of Eqs. (27–30), by means of conditions (31) and Eqs. (35) and (36), yields

$$\xi_1(x_1) = -\frac{k^2}{\lambda_1^2}x_1 - \frac{1}{2}\int_0^{x_1} w_1'^2\, dx_1 \tag{40}$$

$$\xi_2(x_2) = C - \frac{1}{2}\int_0^{x_2} w_2'^2\, dx_2 \tag{41}$$

$$w_1(x_1) = C_1 \sin kx_1 + C_3 x_1 \tag{42}$$

$$w_2(x_2) = \bar{C}_1 x_2^3 + \bar{C}_3 x_2 \tag{43}$$

where C_1, $\bar{C}_1$, C_3, and $\bar{C}_3$ are integration constants to be determined and C represents the horizontal displacement of the movable hinge; consequently, $\xi_2(x_2)$ represents the absolute axial displacement, which is equal to the relative axial displacement of the bar plus the horizontal displacement of the movable support. As is shown subsequently, the constant C does not influence the nonlinear equilibrium path and, therefore, the critical load. From conditions (34) and (39), it is found that

$$C_1 = \frac{\rho[k^2 + \beta^2(e-1)]}{k^2 \sin k} \tag{44}$$

$$\bar{C}_1 = \frac{\rho^2(k^2 - \beta^2)}{6\mu} \tag{45}$$

$$C_3 = 0 \tag{46}$$

$$\bar{C}_3 = \frac{\rho[k^2 + \beta^2(e-1)]}{k\tan k} - \frac{\rho^2(k^2 - \beta^2)}{2\mu} \tag{47}$$

By means of relations (44–47) and Eqs. (40–43), condition (33) leads to the following nonlinear equilibrium equation:

$$\frac{\rho(\beta^2 - k^2)}{3\mu} + \frac{k^2 + \beta^2(e-1)}{k\tan k} - \frac{k^2}{\rho^2\lambda_1^2} - \left[\frac{k^2 + \beta^2(e-1)}{2k\sin k}\right]^2 \times \left(1 + \frac{\sin 2k}{2k}\right) = 0 \tag{48}$$

This equation is independent of the constant C and, therefore, of relation (32). By solving Eq. (48) numerically with respect to k for different levels of the load β^2 and various values of the parameters λ_1, ρ, μ, and e, one can establish the entire (prebuckling and postbuckling) equilibrium path. Thus, from Eqs. (40) and (42), using Eqs. (44) and (46), we obtain the following joint displacement components:

$$\xi_1(1) = -\frac{k^2}{\lambda_1^2} - \rho^2\left[\frac{k^2 + \beta^2(e-1)}{2k\sin k}\right]^2\left(1 + \frac{\sin 2k}{2k}\right) \tag{49}$$

$$w_1(1) = (\rho/k^2)[k^2 + \beta^2(e-1)] \tag{50}$$

$$w_1'(1) = \frac{\rho\cot k}{k}[k^2 + \beta^2(e-1)] \tag{51}$$

As mentioned earlier, Eq. (48) is independent of condition (32), i.e., $w_1(1) = \rho\xi_2(1)$, which serves only for determining the horizontal translation of the movable hinge. The axial displacement $\xi_1(x_1)$, determined by Eq. (40), consists of two component parts. The first part, which is linear with respect to k^2, represents the shortening of the centerline of the column due to axial displacement. The second part of the axial displacement, i.e., the integral, is due to bending of the column centerline and is nonlinear with respect to k^2. The last two terms in the equilibrium equation (48) evidently correspond to the foregoing two components of the axial displacement. It can be proved that the magnitudes of these two terms are considerably smaller than those of the other two terms of Eq. (48). On the basis of this observation, under certain conditions, either one of these terms can be omitted. Apparently, a considerable simplification of Eq. (48) is obtained by neglecting the nonlinear (integral) term in the axial displacement $\xi_1(x)$ given by Eq. (40). On the other hand, the linear term in the axial displacement can be neglected in the case of large values of the length ratio ρ and/or large values of the slenderness ratio λ_1 [see Eq. (48)].

In view of the preceding development, one can establish a simplified nonlinear stability analysis that is associated with the following kinematic continuity conditions:

$$w_2(1) = (1/\rho)\left(k^2/\lambda_1^2\right) \tag{52}$$

$$w_2(1) = -\frac{1}{2\rho}\int_0^1 w_1'^2\, dx_1 \tag{53}$$

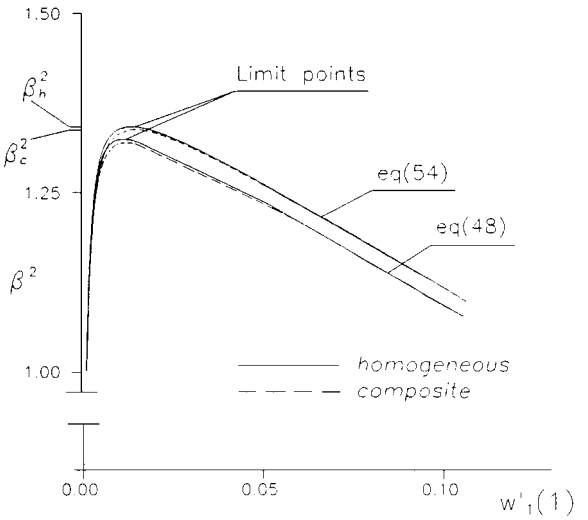

Fig. 7 Equilibrium paths on the basis of the simplified and the accurate nonlinear analysis for $e = 0$, $(\lambda_1)_h = 40$, and $\rho = \mu = 1$ homogeneous frame and $(\lambda_1)_c = 37.91$ composite frame.

On the basis of Eq. (52), one can find for $e = 0$ the following nonlinear equilibrium equation:

$$\frac{k^2}{\rho^2\lambda_1^2} = \frac{\rho}{3\mu}(k^2 - \beta^2)\left(\frac{3\mu}{\rho k \tan k} - 1\right) \tag{54}$$

Subsequently, it is deduced that condition (53) is valid only for large values of ρ and/or λ_1, whereas condition (52) holds practically for all values of λ_1 and/or ρ.

Nonlinear equilibrium equation (48), as well as either one of its invariants, can be written in the form

$$F(k;\, \beta) = 0 \tag{55}$$

This equation can be solved, at least implicitly, leading to

$$\beta = \beta(k) \tag{56}$$

Substituting $\beta(k)$ into Eq. (55) yields the identity

$$F[k,\, \beta(k)] \equiv 0 \tag{57}$$

which upon differentiation gives

$$F_k + F_\beta \frac{\mathrm{d}\beta}{\mathrm{d}k} = 0 \tag{58a}$$

or

$$\frac{\mathrm{d}\beta}{\mathrm{d}k} = -\frac{F_k}{F_\beta} \qquad (F_\beta \neq 0) \tag{58b}$$

The limit point load corresponds to a maximum of the curve β vs k, and therefore a necessary condition for its evaluation is

$$\frac{\mathrm{d}\beta}{\mathrm{d}k} = 0 \qquad \text{or} \qquad F_k(k,\, \beta) = 0 \tag{59}$$

Thus, the critical load is obtained by solving the system of equations

$$F(k,\, \beta) = 0 \qquad \text{or} \qquad F_k(k,\, \beta) = 0 \tag{60}$$

The solution $(k_{\mathrm{cr}},\, \beta_{\mathrm{cr}})$ of this system corresponds to the limit point (Fig. 7), which can be viewed as the point of intersection of the two curves given in Eq. (60). Because we are looking for a maximum, $\mathrm{d}^2\beta/\mathrm{d}k^2 < 0$ or, by means of relation (58),

$$F_{kk}(k_{\mathrm{cr}},\, \beta_{\mathrm{cr}}) > 0 \tag{61}$$

Note also that β_{cr} is the smallest (positive) load for which the system of Eq. (60) is fulfilled. Condition (59), together with condition (61), defines stability criteria.

Numerical Results and Discussion

As a first example, consider the pultruded I beam shown in Fig. 3. The layup for the flanges and the web are shown in Figs. 3a and 3b,

Table 1 Micromechanical data for the 15 × 15 cm I beam[a] shown in Fig. 3

Layer	E_1, MPa	E_2, MPa	ν_{12}	G_{12}, MPa	ν_f, %
Nexus	6,187	6,187	0.40	2,214	10
Continuous strand mat	9,925	9,925	0.42	3,490	23
Roving 1	15,808	4,076	0.25	1,662	18
Roving 2	39,278	6,704	0.27	2,724	52
Roving 3	24,781	4,793	0.26	1,952	31
Roving 4	37,209	6,338	0.27	2,579	49
Roving 5	35,140	6,021	0.27	2,448	46

[a]The information shown corresponds to material not currently produced and is not representative of current structural shapes.

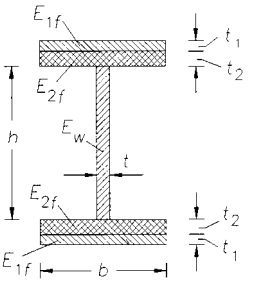

Fig. 8 Composite I-beam cross section: geometric and material characteristics.

respectively. Considering transverse isotropy on each layer,[8] four material properties per layer must be determined. Using micromechanics, the material properties $(E_1, E_2, \nu_{12}, G_{12})$ are determined for each layer from the material properties of fiber (E_f, ν_f) and matrix (E_m, ν_m) (see Fig. 2). For E-glass fibers it is $E_f = 72{,}393$ MPa and $\nu_f = 0.22$, whereas for a vinylester matrix it is $E_m = 3445$ MPa and $\nu_m = 0.35$. As an example, consider an E-glass-vinylester pultruded material with $\nu_f = 0.25$ for which we obtain $E_1 = 20{,}632$ MPa, $E_2 = 4433$ MPa, and $\nu_{12} = 0.318$. The elasticity solution with contiguity is used for the determination of the shear modulus. Using Eq. (3.68) of Ref. 8, one can obtain $G_{12} = 1985$ MPa. The predicted value does not correlate well with experimental data.[24] Therefore, the stress partition parameter[9] is obtained using experimental data for currently produced pultruded material and it is assumed to remain constant while varying the fiber volume and resin properties during material optimization studies. Predictions using this approach correlate well with experimental data.[24]

The micromechanical properties of the pultruded composite beam shown in Fig. 3 are presented in Table 1. Regarding the nexus layers that fall into the category of unidirectional composites, Eq. (9) has been used to compute the micromechanical properties. A buckling analysis of composite columns or frames can be readily performed.

From the postbuckling analyses presented for the cases of a bar and a simple two-bar frame made of composite materials, it is easily concluded that the only parameters affecting the critical load k^2 and the postbuckling path (corresponding to an overall buckling mode) are the axial and bending stiffness A and D of the considered cross section. The cross section (flanges–web) may be composed of many layers, each one contributing to the total bending stiffness. Each layer is made of a homogeneous material or a material with characteristic properties equivalent to a homogeneous material.

A parametric study of the variation of the bending stiffness is performed for the case of an I-beam cross section, where the flange is composed by two different material layers and the web by a third material (Fig. 8). The parameters considered in the evaluation of the axial and bending stiffness are the flange width b; the thicknesses of each layer of the flange, namely, t_1 and t_2; the height of the web h; and the thickness t of the web. Each layer is made of an isotropic material with modulus of elasticity E_{1f} and E_{2f} for the flanges and E_w for the web, respectively. The axial stiffness A_h of an I-beam made of a homogeneous material $E = E_w$ is

$$A_h = [th + 2b(t_1 + t_2)]E_w \tag{62}$$

On the other hand, the axial stiffness A_c of the composite I beam with various materials is

$$A_c = thE_w + 2b(t_1E_{1f} + t_2E_{2f}) \tag{63}$$

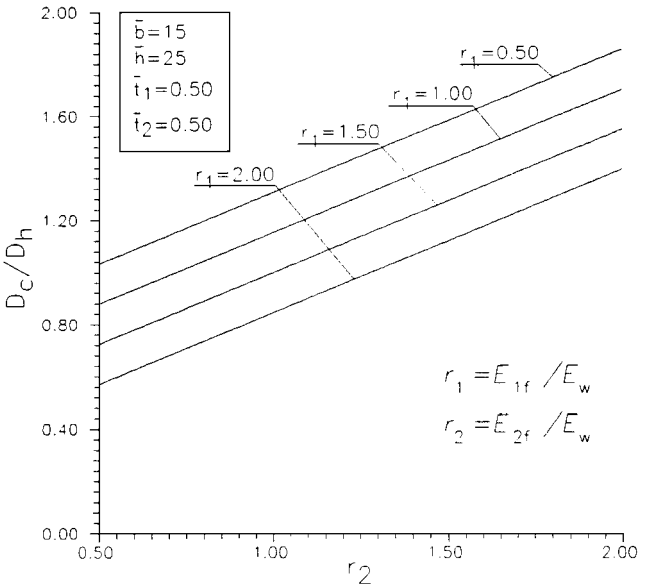

a) Various values of r_1

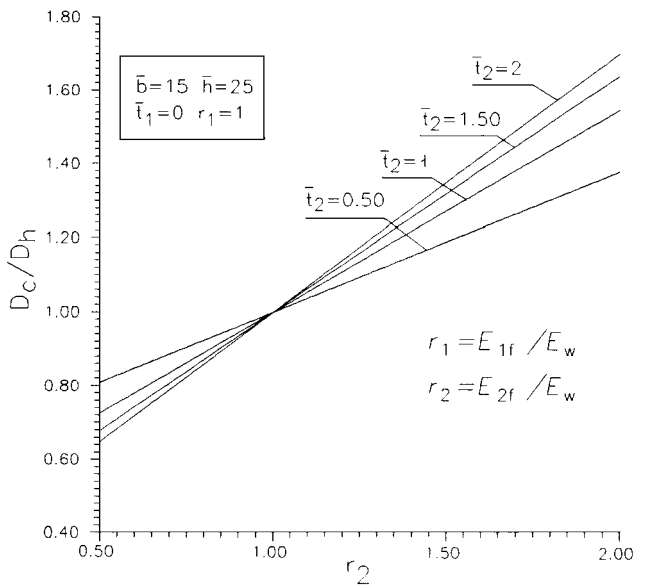

b) Various values of $\bar{t}_2$

Fig. 9 Bending stiffness fraction D_c/D_h vs r_2.

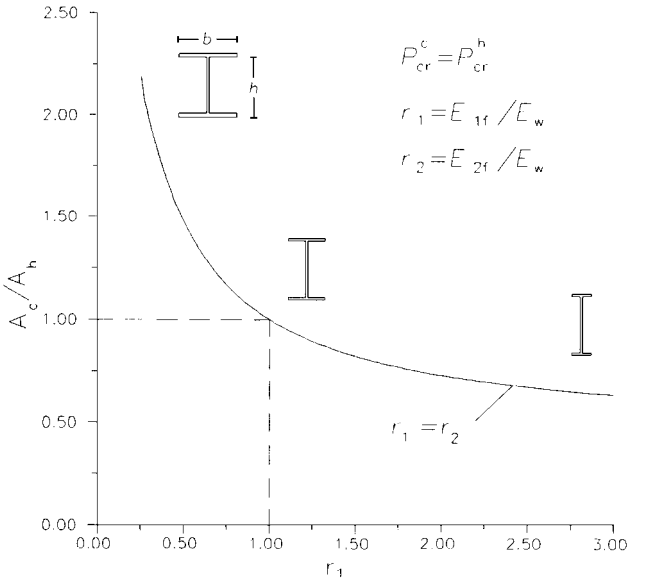

Fig. 10 Stiffness ratio A_c/A_h vs strength ratio r_1 for $P^h_{cr} = P^c_{cr}$.

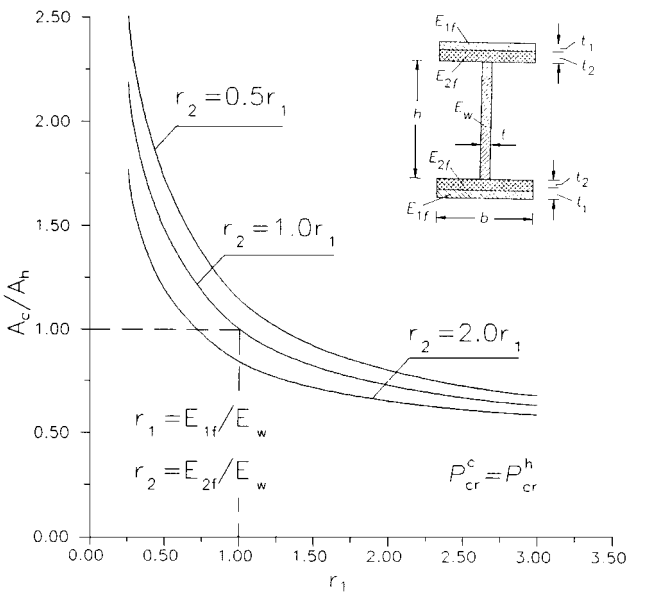

Fig. 11 Area ratio A_c/A_h vs strength ratio r_1 for $P^h_{cr} = P^c_{cr}$.

Using the nondimensional quantities $\bar{t}_1$, $\bar{t}_2$, $\bar{b}$, and r_1 and r_2, where $\bar{t}_1 = t_1/t$, $\bar{t}_2 = t_2/t$, $\bar{b} = b/t$, $\bar{h} = h/t$, $r_1 = E_{1f}/E_w$, and $r_2 = E_{2f}/E_w$, we can compute the axial stiffness fraction A_c/A_h as follows:

$$\frac{A_c}{A_h} = \frac{\bar{h} + 2\bar{b}(\bar{t}_1 r_1 + \bar{t}_2 r_2)}{\bar{h} + 2\bar{b}(\bar{t}_1 + \bar{t}_2)} \tag{64}$$

Similarly, the bending stiffness D_h of an I beam made of a homogeneous material E_w is

$$D_h = \left[\tfrac{1}{6}b(t_1+t_2)^3 + \tfrac{1}{12}th^3 + \tfrac{1}{2}b(t_1+t_2)(h+t_1+t_2)^2\right]E_w \tag{65}$$

and the bending stiffness D_c of the composite I beam with various materials is

$$D_c = \tfrac{1}{6}bt_1^3E_{1f} + \tfrac{1}{6}bt_2^3E_{2f} + \tfrac{1}{12}th^3E_w + 2bt_1E_{1f}\left(\tfrac{1}{2}h + t_2 + \tfrac{1}{2}t_1\right)^2 + \tfrac{1}{2}bt_2E_{2f}(h+t_2)^2 \tag{66}$$

The bending stiffness fraction is

$$\frac{D_c}{D_h} = \frac{\frac{1}{6}\bar{b}\left(r_1\bar{t}_1^3 + r_2\bar{t}_2^3\right) + \frac{1}{12}\bar{h}^3 + 2\bar{b}\bar{t}_1 r_1\left(\frac{1}{2}\bar{h} + \bar{t}_2 + \frac{1}{2}\bar{t}_1\right)^2 + \frac{1}{2}\bar{b}\bar{t}_2 r_2(\bar{h}+\bar{t}_2)^2}{\frac{1}{6}\bar{b}(\bar{t}_1+\bar{t}_2)^3 + \frac{1}{12}\bar{h}^3 + \frac{1}{2}\bar{b}(\bar{t}_1+\bar{t}_2)(\bar{h}+\bar{t}_1+\bar{t}_2)^2} \tag{67}$$

The bending stiffness D_c corresponding to the composite I beam is compared with D_h of the homogeneous I beam. For various values of the parameters $\bar{t}_1$, $\bar{t}_2$, $\bar{b}$, $\bar{h}$, r_1, and r_2, the stiffness fraction Eq. (67) is varying linearly as shown in Figs. 9a and 9b. As a demonstrative example, the postbuckling behavior of the frame shown in Fig. 6 composed of I-beam members with various values of $r_1 = r_2$ is compared with the postbuckling behavior of the frame with homogeneous I-beam members for which $r_1 = r_2 = 1$ and $(\lambda_1)_h = 40$, whereas all of the other parameters are $\bar{t}_1 = 0.5$, $\bar{t}_2 = 0.5$, $\bar{b} = 15$, and $\bar{h} = 25$. Using Eq. (64), we obtain the axial stiffness fraction A_c/A_h and by Eq. (67) the bending stiffness fraction D_c/D_h. Thus, for the composite frame we compute the slenderness $(\lambda_1)_c$ and the critical load P^c_{cr}. The postbuckling paths for the homogeneous and the composite frame with $r_1 = r_2 = 1.25$ and $(\lambda_1)_c = 37.91$ are both drawn in Fig. 7 for comparison, using Eqs. (48) and (54). Next, we vary the flange width b as well as the modulus ratios r_1 and r_2, and we determine the cross-sectional area for which $P^c_{cr} = P^h_{cr}$. This can be translated to weight-to-strength curves shown in Figs. 10 and 11. It is clear that, if the flanges are made from strong material compared

with the web, we can achieve as much as a 35% reduction of the material, whereas the situation is badly reversed in the case of weak flanges and strong web.

The methodology may apply to cases of cross sections made of any composite material, such as fiber-reinforced plastic beams or steel cross sections with a combination of high- and lower-strength steel layers.

Conclusions

The most important conclusions based on the models discussed are the following.

1) A comprehensive analysis, starting from the properties of the composite material and leading to the determination of the critical buckling load and the postbuckling behavior, that can be used by the manufacturer to tailor the material properties for specific applications has been developed. The analytical solution presented herein can be used to predict the critical buckling load as well as the postbuckling behavior of commercially available pultruded columns.

2) The postcritical response of a simply supported bar and a two-bar frame can be readily established. More specifically, a linearized analysis with nonlinear bending–moment curvature relationship is performed for the bar, whereas for the two-bar frame a postbuckling analysis associated with nonlinear kinematic relationship and a linear bending–moment curvature relation is established.

3) Stability criteria for a direct determination of the critical loads are also presented.

4) A simplified and effective technique (with linear bending moment–curvature and linear kinematic relations) can be used for the approximate evaluation of the postbuckling behavior.

5) The axial and bending stiffnesses of a composite member are the only parameters affecting the critical buckling load and postbuckling behavior.

6) The individual and combined effect of the geometric and material properties on the load-carrying capacity of columns and frames is highlighted through the parametric study presented.

References

[1]*Creative Pultrusions Design Guide*, Creative Pultrusions, Inc., Pleasantville Industrial Park, Alum Bank, PA, 1994.

[2]Barbero, E. J., and Raftoyiannis, I. G., "Buckling Analysis of Pultruded Composite Columns," *Impact and Buckling of Structures*, edited by D. Hui, ASME AD-Vol. 20, AMD-Vol. 114, American Society of Mechanical Engineers, New York, 1990, pp. 47–52.

[3]Barbero, E. J., and Raftoyiannis, I. G., "Local Buckling of FRP Beams and Columns," *ASCE Journal of Materials in Civil Engineering*, Vol. 5, No. 3, 1993, pp. 339–355.

[4]Barbero, E. J., and Reddy, J. N., "Modeling of Delamination in Composite Laminates Using a Layer-Wise Plate Theory," *International Journal of Solid Structures*, Vol. 28, No. 3, 1991, pp. 373–388.

[5]Chamis, C. C., "Micromechanics Strength Theories," *Composite Materials*, edited by L. J. Broutman, Vol. 5, Fracture and Fatigue, Academic, New York, 1974, Chap. 3.

[6]Simitses, G. J., "Effect on Delamination on Buckling," *Key Engineering Materials*, Vol. 37, 1989, pp. 237–251.

[7]Simitses, G. J., Chen, Z. Q., and Sallam, S., "Delamination Buckling of Cylindrical Laminates," *Thin-Walled Structures*, Vol. 11, Nos. 1, 2, 1991, pp. 25–41.

[8]Jones, R. M., *Mechanics of Composite Materials*, Hemisphere, New York, 1975.

[9]Tsai, S. W., and Hahn, H. T., *Introduction to Composite Materials*, Technomic, Lancaster, PA, 1980.

[10]Bank, L. C., "Flexural and Shear Moduli of Full-Section Fiber Reinforced Plastic (FRP) Pultruded Beams," *Journal of Testing and Evaluation*, Vol. 17, No. 1, 1989, pp. 40–45.

[11]Bank, L. C., "Shear Coefficients for Thin-Walled Composite Beams," *Computers and Structures*, Vol. 8, 1987, pp. 47–61.

[12]Barbero, E J., and Raftoyiannis, I. G., "Euler Buckling of Pultruded Composite Columns," *Composite Structures*, Vol. 24, 1993, pp. 139–147.

[13]Bleich, F., *Buckling Strength of Metal Structures*, McGraw–Hill, New York, 1952.

[14]Huchinson, J. R., and Koiter, W. T., "Post-Buckling Theory," *Applied Mechanics Review*, Vol. 23, 1970, pp. 1353–1366.

[15]Koiter, W. T., "On the Stability of Elastic Equilibrium," Ph.D. Thesis, Delft Univ., Delft, The Netherlands, 1945; see also NASA TT-F 10,833, 1967.

[16]Kounadis, A. N., Giri, J., and Simitses, G. J., "Nonlinear Stability Analysis of an Eccentrically Loaded Two-Bar Frame," *Journal of Applied Mechanics*, Vol. 44, No. E4, 1977, pp. 701–706.

[17]Simitses, G. J., and Kounadis, A. N., "Buckling of Imperfect Rigid-Jointed Frames," *Journal of Engineering Mechanics*, Vol. 104, EM3, 1978, pp. 569–586.

[18]Vinson, J. R., and Sierakowski, R. L., *The Behavior of Structures Composed of Composite Materials*, Martinus–Nijhoff, Dordrecht, The Netherlands, 1987.

[19]Tsai, S. W., *Composites Design*, 4th ed., Think Composites, Dayton, OH, 1989.

[20]Berkowitz, H. M., "A Theory of Simple Beams and Columns for Anisotropic Materials," *Journal of Composite Materials*, Vol. 3, 1969, pp. 196–200.

[21]Naughton, B. P., Panhuizen, F., and Venmeulen, A. C., "The Elastic Properties of Chopped Strand Mat and Woven Roving in g.r. Laminae," *Journal of Reinforced Plastics Composites*, Vol. 4, No. 2, 1985, pp. 195–204.

[22]Thompson, J. M., and Hunt, G. W., *A General Theory of Elastic Stability*, Wiley, New York, 1973, p. 28.

[23]Kounadis, A. N., "An Efficient Simplified Approach for the Nonlinear Buckling Analysis of Frames," *AIAA Journal*, Vol. 23, No. 8, 1985, pp. 1254–1259.

[24]Barbero, E. J., and Sonti, S. S., "Micro-Mechanical Modeling of Pultruded Composite Beams," *Proceedings of the AIAA 32nd Structures, Structural Dynamics, and Materials Conference*, CP 911, AIAA, Washington, DC, 1991, AIAA Paper 91-1045.

G. A. Kardomateas
Associate Editor